Inkjet printed chemical sensor array based on polythiophene conductive polymers

Bo Li [a], Suresh Santhanam [a], Lawrence Schultz [b], Malika Jeffries-EL [c], Mihaela C. Iovu [c], Genevieve Sauvé [c], Jessica Cooper [c], Rui Zhang [c], Joseph C. Revelli [d], Aaron G. Kusne [a], Jay L. Snyder [d], Tomasz Kowalewski [c], Lee E. Weiss [b], Richard D. McCullough [c], Gary K. Fedder [a], David N. Lambeth [a,*]

[a] *Department of Electrical and Computer Engineering, Carnegie Mellon University, Pittsburgh, PA 15213, USA*
[b] *Robotics Institute, Carnegie Mellon University, Pittsburgh, PA 15213, USA*
[c] *Department of Chemistry, Carnegie Mellon University, Pittsburgh, PA 15213, USA*
[d] *National Personal Protective Technology Laboratory, National Institute for Occupational Safety and Health, Pittsburgh, PA 15236, USA*

Abstract

Multiple regioregular polythiophene polymers with a variety of side chains, end groups and secondary polymer chains were used as active sensing layers in a single chip chemresistor sensor array device. A custom inkjet system was used to selectively deposit the polymers onto the array of transduction electrodes. The sensor demonstrated sensitivity and selectivity for detection and discrimination of volatile organic compounds (VOCs). The conductivity responses to VOC vapors are dependent on the chemical structure of the polymers. For certain VOCs, conductivity increased in some polymers, while it decreased in others. Principal component analysis (PCA) of sensor responses was used to discriminate between the tested VOCs. These results are correlated to the chemical structures of the different polymers, and qualitative hypothesis of chemical sensing mechanisms are proposed. This research demonstrates the potential for using such devices in VOC detection and discrimination sensing applications.
© 2006 Elsevier B.V. All rights reserved.

Keywords: Chemresistor; Gas sensing; Inkjet printing; Polythiophene; Volatile organic compounds

1. Introduction

The development of a low cost, low power and portable device for detection and identification of volatile organic compounds (VOCs) is needed for applications such as homeland security and monitoring of agriculture, medical, and manufacturing environments [1–9]. One of the most difficult challenges is to find sensing materials that have good sensitivity and robust selectivity to the substances to be detected. While there has been some success in sensor development for greenhouse gases (CO_2, CH_4, N_2O, NO and CO), the technology for the detection of VOCs remains challenging due to the similarities in chemical composition and structure between the small VOC molecules. For one example, semiconducting metal oxide sensors, which are based on chemical oxidizing and reduc-

ing reactions between the oxygen ion and analytes at elevated temperatures (300–500 °C) [1,10], are limited because VOCs generally have similar reducing reaction energies. For another example, carbon black composite materials operate based on swelling of the polymers by the absorbed analytes, which increases the space between carbon particles, leading to a decrease in conductivity upon exposure to VOCs [7,11]. This percolation-based sensing mechanism has been a limiting factor for these materials because it is restricted to a single sensing modality that has similar responses to many VOCs.

Conductive conjugated polymers are a relatively new class of VOC sensing materials that show considerable promise to overcome these limitations. First, their chemical composition is similar to VOCs, which may induce physical interactions between sensing materials and analytes, leading to new sensing mechanisms [2]. Second, their chemical structures are readily modified, which enables custom material designs with specific selectivity to target analytes. And third, unlike the semiconducting metal oxide sensors, the sensing operation occurs

* Corresponding author. Tel.: +1 412 268 3674; fax: ++1 412 268 4916.
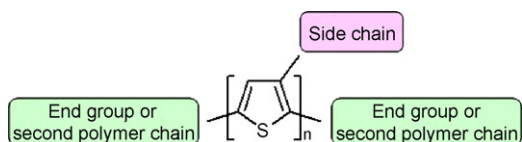*E-mail address:* lambeth@ece.cmu.edu (D.N. Lambeth).

Fig. 1. Schematic diagram of regioregular polythiophene based polymers.

at room temperature, which lowers the power consumption requirements.

For example, regioregular polythiophenes (rr-PTs) polymers have an air-stable conducting property that makes them suitable as chemresistive sensing materials. Their solubility in a variety of organic solvents also enables them to be inkjet printed for device fabrication [12,13]. Fig. 1 shows the general chemical structure of the regioregular polythiophenes. The backbone of the polymer is formed by thiophene rings. A chemical side-chain group can be attached on each thiophene ring along the polymer and an end-group or a secondary copolymer chain can be added to each end of the polythiophene. This variety of possible structures enables a potentially broad library of candidate materials for VOC sensing. Combinatorial analysis of sensor arrays

incorporating these multi-materials has the potential to provide robust and selective detection of VOCs via the 'electronic nose' concept [7].

In the work reported here, nine regioregular polythiophene-based polymers with different side chains, end-groups and copolymers were characterized for their conductance responses to 10 different VOCs. The materials, device construction, and testing procedure are described, and then correlation between conductivity responses, analytes properties and polymer chemical structures are discussed. Lastly, possible sensing mechanisms involving different physical interactions between analytes and polymer molecules are proposed.

2. Experimental

2.1. Materials

The rr-PTs polymers used in this study were synthesized using methods previously described [14–18]. The chemical structures and properties of these polymers are shown in Table 1. Poly(3-hexylthiophene) (P3HT) was used as a reference

Table 1
Chemical structures and properties of thiophene based polymers

Polymer	Chemical structure	Composition[a]	Molecular weight[b]	PDI[b]
Poly(3-hexylthiophene) (P3HT)		100 mol% P3HT	11600	1.2
Poly(3-dodecylthiophene) (PDDT)		100 mol% PDDT	47352	1.2
Poly(3-methoxyethoxy-ethoxymethyl)thiophene (PMEEM)		100 mol% PMEEM	N/A	N/A
Bromoester terminated poly(3-hexylthiophene) (P3HT-bromoester)		100 mol% P3HT	11200	1.2
Benzyl terminated Poly(3-hexylthiophene) (P3HT-benzyl)		100 mol% P3HT	13670	1.2
Poly(3-hexylthiophene)-*b*-polystyrene (P3HT-*b*-PS)		65 mol% P3HT	16500	1.3
Poly(3-hexylthiophene)-*b*-poly(methylacrylate) (P3HT-*b*-PMA)		80 mol% P3HT	14620	1.2
Poly(hexylthiophene)-*b*-poly(butylacrylate) (P3HT-PBA)		82 mol% P3HT	16000	1.2
Poly(3-dodecylthiophene-*ran*-3-methylthiophene) (PDDT-*r*-PMT)		50 mol % PDDT	11950	1.2

[a] Mole percentage of PHT composition was determined by ^{1}H NMR spectroscopy.
[b] Number average molecular weight and polydispersity were determined by GPC with polystyrene as standard.

polymer since it and its properties have been discussed in the literature [19–21]. P3HT, poly(3-dodecylthiophene) (PDDT) and poly(3-methoxyethoxyethoxymethyl)thiophene (PMEEM) are polythiophene polymers with different side chains. P3HT, benzyl terminated P3HT (P3HT-benzyl), and bromoester terminated P3HT (P3HT-bromoester) are polythiophene polymers with different end groups. Poly(3-hexylthiophene)-*b*-polystyrene (P3HT-*b*-PS), poly(3-hexylthiophene)-*b*-poly(butylacrylate) (P3HT-*b*-PBA), and poly(3-hexylthiophene)-*b*-poly(methylacrylate) (P3HT-*b*-PMA) are polythiophene-based block copolymers with different secondary polymer chains. And, poly(3-dodecylthiophene-*ran*-methylthiophene) (PDDT-*r*-PMT) is a random copolymer with a different secondary polymer chain randomly inserted into the primary polythiophene chain. To form inks for inkjet deposition, the polymers were dissolved in trichlorobenzene at 5 mg/ml concentration and then filtered with a 0.4 μm PTFE syringe filter.

2.2. Sensor array

2.2.1. Sensor design

The sensor array consists of 24 sensor elements in a 4×6 matrix, as shown in Fig. 2(a). Each sensor element uses two concentric spiral electrodes (Fig. 2(b)) to measure polymer con-
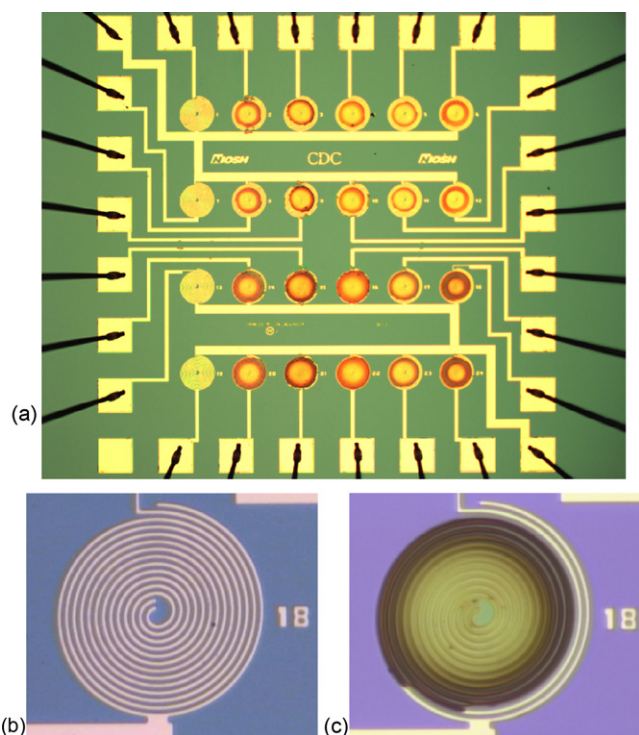

Fig. 2. Optical micrograph of sensor arrays. (a) Completed, wire bonded, test chip showing 24 electrode patterns with ink-jetted polymers on 20 of these. The sensors in the first column were used for reference. The rest of the electrodes have one type polymer jetted on each column. From left to right, the polymers are poly(3-hexylthiophene)-*b*-polystyrene), poly(hexylthiophene)-*b*-poly(butylacrylate), poly(3-methoxyethoxyethoxymethyl)thiophene, poly(3-dodecylthiophene-*ran*-3-methylthiophene), poly(3-hexylthiophene)-*b*-poly-(methylacrylate). (b) Enlarge view of the gold spiral electrodes with no polymer. (c) Spiral electrodes with jetted poly(3-hexylthiophene) polymer formed from 10 drops of 5 mg/mL polymer concentration dissolved in trichlorobenzene.

ductance. One electrode is connected to a common power bus and the other is dedicated to the particular element. The gap between the electrodes forms the active sensing area. The spiral electrode geometry maximizes the sensing area per overall sensor size. The diameter of the spiral electrodes is 200 μm; the gap is 3 μm; the width of the electrode metal is 4 μm; the total length of the electrodes is around 4 mm. Hence, each sensor element is approximately 200 μm in diameter and the overall test chip is 3 mm × 3 mm in size.

2.2.2. Sensor fabrication

Sensors were prepared on conductive *n* + silicon substrates with a thermally grown 700 nm insulating SiO$_2$ surface. The fabrication process requires two masks. A 5 nm layer of Ti covered by a 50 nm layer of Au was sputter deposited and patterned as the electrodes using the first mask. The Ti layer was used to improve the adhesion of Au to the silicon dioxide layer. The Au layer was used as the contact layer to interface to the polythiophene polymers. The work function of Au matches the ionization potential of polythiophenes; therefore, it tends to form an ohmic contact between electrodes and polymers [22]. The second mask was used to deposit an additional 1 μm of Au onto the bonding pad area to make it more robust.

There are several requirements for polymer deposition. First, multiple polymer solutions must be selectively deposited onto a single sensor chip to provide combinatorial sensing responses. Second, due to the small size of each sensor element, the deposition process must be able to control picoliter solution volumes. Third, the targeting accuracy for depositing the polymer onto each element must be within a few microns. Inkjet deposition satisfies these requirements. It is a versatile, cost-effective, and programmable approach that has been used for a range of other organic electronic manufacturing applications, including organic thin-film transistors, organic light-emitting diodes, and other sensors [23,24]. A custom inkjet deposition system was designed and constructed in order to have complete control over the jetting parameters, deposition sequence, and targeting accuracy. With the aid of computer vision-based calibration, a targeting accuracy of ±4 μm or less was achieved. The inkjet system can deposit 50 pL droplets using an OEM drop-on-demand printhead with a 30 μm diameter nozzle (Microfab, Inc., Plano, TX). The details of our inkjet system and the deposition process are described in detail in [25]. For example, Fig. 2(a) shows a fabricated sensor integrating multiple deposited polymers on the electrode site array. Fig. 2(b) and (c) show a sensor element before and after polymer deposition, respectively. Sensor data in the results section are given for devices printed with 10 sequential drops on each element. After polymer jetting, the sensors were vacuum annealed at 100 °C for 12 h to drive off any remaining solvent.

2.3. Sensor testing

Fig. 3 shows a schematic of the computer-controlled testing system. A nitrogen gas supply is split into two gas branches. One is the carrier gas stream. The other branch flows through an analyte bubbler and generates saturated analyte vapor, which is
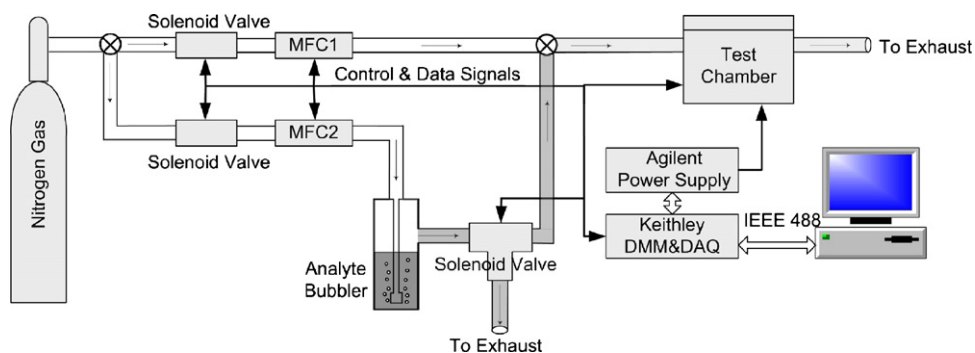
Fig. 3. Block diagram of computer controlled chemical vapor testing system.

later mixed with the carrier nitrogen stream to achieve the desired analyte concentration. Two mass flow controllers are used to control the gas flow of these branches. The carrier gas stream is set at 1 L/min, and the analyte vapor flow can be adjusted from 0 to 10 mL/min for different analyte concentrations. The analyte vapor is directed to either the sensor test chamber or an exhaust by a three-way solenoid valve. The time delay for analyte vapor arriving at the test vessel is around 20 s for the lowest analyte vapor flow. All the solenoid valves and mass flow controllers are controlled by a Keithley 7706 DAQ card installed inside the Keithley 2700 digital multimeter.

Fabricated sensors were mounted in 40-pin DIP packages and then plugged into a custom printed circuit board (PCB) mounted inside of an aluminum test chamber with a volume of less than 5 in.^{3}. The PCB contains signal amplification and multiplexing electronics. An Agilent E3647A dual output DC power supply supplies the proper DC voltages to the PCB electronics and sensor electrodes. The amplified sensor signals are acquired by the Keithley 2700 multimeter. The entire system is controlled over an IEEE 488 control bus using a custom Labview program.

In this study, six polar VOC vapors (methanol, ethanol, isopropanol, acetone, methylene chloride, and acetonitrile) and four non-polar vapors (hexane, cyclohexane, toluene and benzene) were tested. The analytes were introduced into the continuous carrier gas flow to the sensor test chamber with a schedule of 10 min on and 10 min off. Care was taken to ensure that the total gas flow rate during testing was a constant. Sequential pulses of five or six concentrations were tested for each VOC vapor by ramping up from a low analyte concentration to a high analyte concentration. The concentration of each vapor at a fixed flow rate depends on its vapor pressure. The concentration of each analyte at each flow rate was accurately measured using a gas chromatography system (Model 8610, SRI Instruments, Inc.). During each test run, the currents flowing through six individual chemresistor sensors were recorded simultaneously at 5 s sampling intervals.

3. Results

3.1. Polymer characterization

Film morphology has an important role in determining the material's sensing properties [26]. This is especially true when comparing the crystalline structures to those of a totally amorphous structure. These variations, such as lattice parameters, porosity, nanostructure geometry, and grain boundary geometry, alter the electrical conduction mechanisms and thus alter the sensitivity, selectivity, and response time for a given analyte.

Prior to using inkjetting to deposit polymers, we used atomic force microscopy (AFM) to investigate the morphology of polymers drop cast from a slowly evaporating solvent onto an oxidized silicon substrate. Our polymers generally showed polycrystalline morphologies. As examples of the observed possible nanostructures, Fig. 4 shows four polymer AFM tapping mode images illustrating nanofibriles and nano-size grains. Other reports [12,27] indicate that, due to the interchain stacking of the polythiophene molecules, dense crystalline nanofibrile structures form from the P3HT homopolymer, and that the electronic properties are correlated to the molecular weight and microstructure. It is reasonable to believe that rr-PTs with different side chains and end groups have different lattice spacing down the length of the nanofibriles, as well as, a varied polycrystalline structure. It is highly likely that the differences in microstructure between these polymers could lead to different VOC sensing behaviors.

Surfaces of deposited inkjetted drops are rougher. It is well known from other inkjet studies that during the fast drying process there is considerable fluid motion [28,29]. In some cases this is so severe that a coffee ring appearance results. Perhaps these dynamics cause the drop roughness and the appearance of an amorphous structure. Hence, the AFM images are less well defined and observation of any distinctive crystalline microstructure is difficult. However, it is conjectured that molecular ordering may exist at least over shorter distances. The relationship between jetting parameters, polymer morphology, and sensing response is currently being investigated and will be discussed in the future. For the remainder of this work all polymers discussed were prepared by ink jetting.

3.2. Sensor array response

Fig. 5 shows the normalized conductance responses over time of different polymers to acetone, methylene chloride, toluene and cyclohexane. Normalization is used to analyze polymer sensor data so that sensors with different base resistances can be compared. The baseline of the sensors also showed drift over
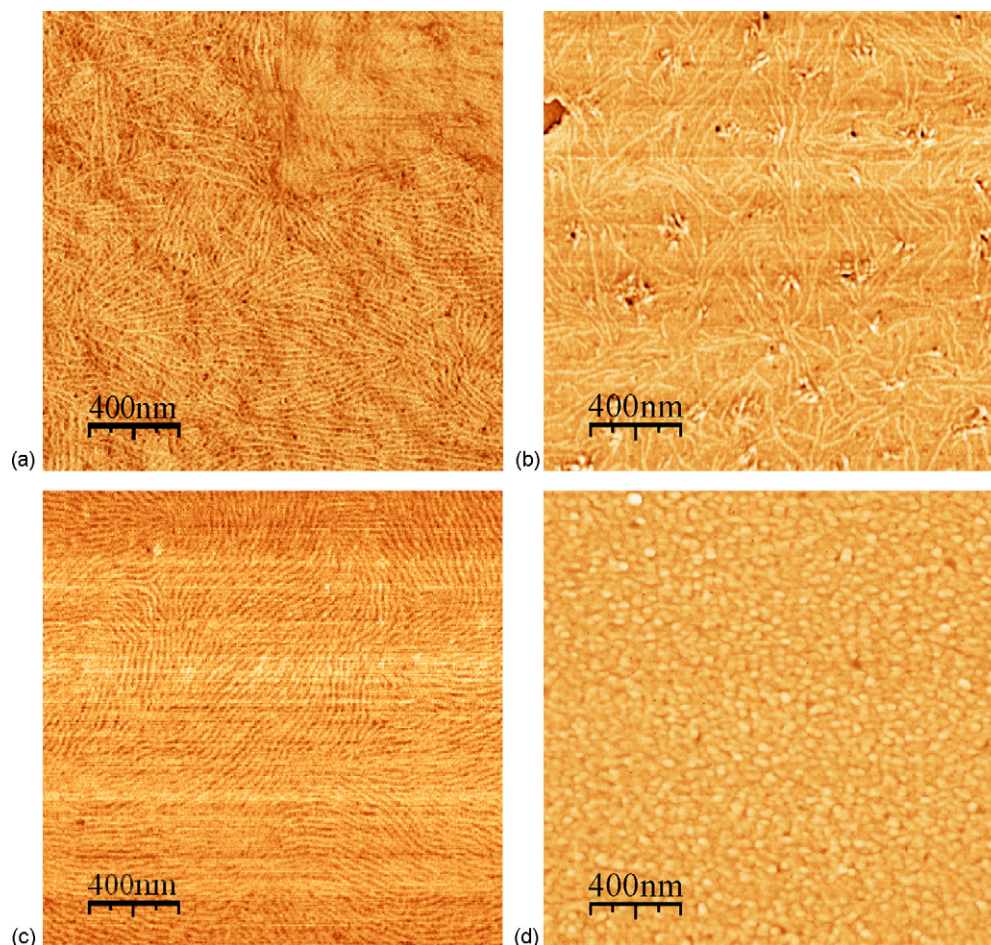
Fig. 4. Tapping mode AFM phase images illustrate the various nanostructures of polymer films made by slow evaporation of the solvent. (a) Poly(3-hexylthiophene). (b) Poly(3-hexylthiophene)-*b*-polystyrene. (c) Poly(hexylthiophene)-*b*-poly(butylacrylate). (d) Poly(3-dodecylthiophene-*ran*-3-methylthiophene).

long periods of time due to temperature variations. A custom Labview program was used to do the normalization and baseline calibration during the measurement. The normalization is based on Eq. (1) in which sensor response is given by

$$G_{\text{response}} = \frac{G_{\text{sens}} - G_0}{G_0} \tag{1}$$

where G_{sens} is the sensor conductance during vapor exposure, and G_0 is the initial conductance. A spline fitting is performed on the baseline data and subtracted to obtain the response curves in Fig. 5. Response sensitivities measured in conductance change per ppm of all tested polymers to 10 VOC vapors are shown in Table 2.

There are several interesting observations from Fig. 5: (1) almost all of the polymers demonstrated a fast chemical response time, with typical rise-times less than 30 s (0–90% of final value); (2) the sensors recovered completely to their baseline after the VOC exposure was removed; (3) with the exception of exposure of P3HT-benzyl to toluene, the sensor responses were nearly linear with analyte concentration; (4) different polymers showed different sensitivity amplitudes; (5) the conductance responses of different polymers can have different signs. For acetone, which is a polar analyte and not a solvent for rr-PTs,

both positive and negative responses were found for the different tested polymers; PMEEM gave the strongest positive response and PDDT-*r*-PMT gave the strongest negative response. For methylene chloride, which is a polar analyte and strong solvent for rr-PTs, all tested polymers showed positive responses, with P3HT being the strongest. For toluene, which is a nonpolar analyte and solvent for rr-PTs, results again showed both positive and negative responses. However, the response pattern is very different from acetone. For toluene, P3HT-benzyl showed the largest positive response. PDDT and PDDT-*r*-PMT showed the largest negative responses. For cyclohexane, which is a non-polar analyte and not a solvent for rr-PTs, all tested polymers showed negative responses, except PMEEM which gave a very small positive response. Here, PDDT showed the strongest negative response.

The complete set of responses of tested polymers, which is shown in Table 2, further illustrates the variety of responses, with different polymers clearly showing a different response pattern. The conductance response amplitude per ppm is on the order of 10^{-6} to 10^{-5}, which is relatively small compared to semiconducting metal oxides [1]; however, it is consistent with other reported sensing results for conductive polymers [3,20].
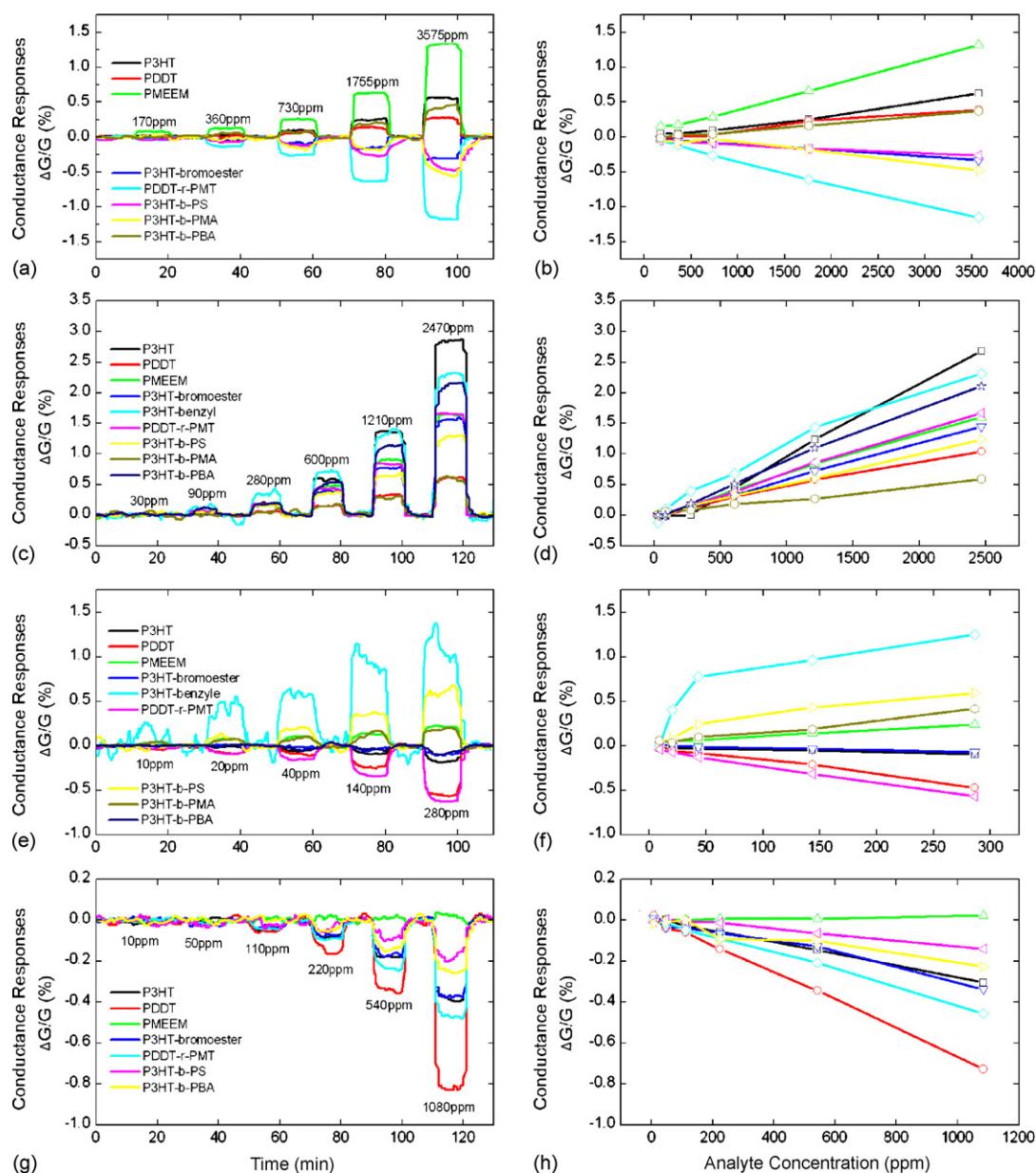
Fig. 5. Sensor responses for various polymers and various VOC vapors. The left column of figures is time response curves while the right column of figures shows the response to concentration. The analytes corresponding to the figures are (a–b) acetone, (c–d) methylene chloride, (e–f) toluene, and (g–h) cyclohexane.

3.3. Principal component analysis

Principal component analysis (PCA) was used to reduce the highly dimensional sensor data into a few uncorrelated dimensions. PCA requires that the exposing analyte concentration for each polymer tested be the same. While our exposure concentrations varied due to the experimental conditions, we can see from Fig. 5, with the possible exception of P3HT-benzyl exposure to toluene, the responses were highly linear with analyte concentration. Hence, we used a linear fit of this data to extrapolate response values of 9 polymers for 10 VOCs at analyte concentration of 200, 400, 600, 800, and 1000 ppm. These response values were then employed in the PCA analysis using XLStat 7.5 (Addinsoft Inc.). The first two principal components F1 and F2 are used as classification vectors. Fig. 6 shows the PCA score plot of 10 analytes.

It can be seen from Fig. 6 that the sensor array response discriminates quite well between some of the VOCs. As anticipated, the score magnitudes linearly increase with analyte concentration. The deviation of the score plots starting at the origin is most likely due to the experimental inaccuracy at very low concentrations. However, for low concentrations the scores for the polar VOCs tend to be clustered in the 1st quadrant, which makes them harder to be identified. The scores for the non-polar vapors are all on the negative half of the F1 axis. It is of interest that the non-polar benzene and toluene, which contain the double bond in the benzene ring, have a positive F2 score while the non-polar non-double bonded ring vapors, hexane and cyclohexane, show

Table 2
Response sensitivity of conductance to different vapors

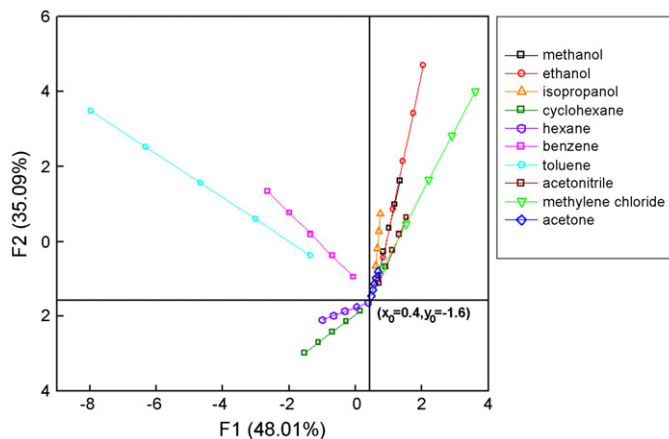| Chemical vapor	μ (D)	P3HT (ppm^{-1} × 10^{-6})	PDDT (ppm^{-1} × 10^{-6})	PMEEM (ppm^{-1} × 10^{-6})	P3HT-bromoester (ppm^{-1} × 10^{-6})	P3HT-benzyl (ppm^{-1} × 10^{-6})	PDDT-r-PMT (ppm^{-1} × 10^{-6})	P3HT-b-PS (ppm^{-1} × 10^{-6})	P3HT-b-PMA (ppm^{-1} × 10^{-6})	P3HT-b-PBA (ppm^{-1} × 10^{-6})
Methanol	1.70	6.39	4.28	6.34	1.59	6.76	−1.75	4.45	−1.25	1.76
Ethanol	1.69	10.5	6.84	11.2	2.54	0.00	−8.05	13.84	−3.72	4.53
Isopropanol	1.58	2.79	0.44	2.75	2.01	−2.88	−5.67	5.79	0.00	1.79
Acetone	2.88	1.25	1.05	3.81	−0.92	0.00	−3.12	−0.76	−1.45	1.04
Methylene chloride	1.60	9.25	4.70	6.26	3.88	9.08	6.64	4.65	2.36	8.27
Acetonitile	3.93	2.48	3.64	10.1	−2.44	6.12	−2.86	−3.67	−4.02	2.69
Toluene	0.38	−1.43	−16.4	8.14	1.22	41.5	−19.6	20.5	14.6	0.00
Benzene	0.00	−1.11	−6.63	6.74	0.69	20.3	−8.42	5.91	2.45	0.00
Hexane	0.00	−1.77	−5.99	1.62	−1.11	0.00	−3.86	0.00	0.00	−1.28
Cylcohexane	0.00	−1.94	−7.13	0.24	−1.59	0.00	−4.24	−1.05	0.00	−1.38

Fig. 6. Principal component score plot of responses of nine polymers to 10 VOC vapors at 200, 400, 600, 800, and 1000 ppm.

a negative F2 score. This leads to a clear discrimination of these analytes.

4. Discussion

The response of this family of rr-PT-based polymers is selective for the range of the VOCs tested. It is inferred that the film microstructure and the molecular structure of these polymers which is related to the different side and end groups have a strong influence on their sensing properties. In general, the sensing behaviors of polymers are related to molecular interactions such as bonding, chemical reactions, dipole interaction and the van der Waals force between the analytes and polymer molecules. For polycrystalline films the behaviors are also related to the microstructure of the material. These interactions possibly modify the charge transportation inside the polymer molecules, or inside the grains, or at the grain boundaries of the nanostructures. At room temperature, phonon-assisted polaron hopping has been proposed to be the conduction mechanism for both inter- and intra-grain charge transportation inside conductive polymers [30]. At the material microstructure level, parameters like film morphology, density and height of grain boundary barrier [31], and density and distribution of delocalized hopping states may determine the current density. At the polymer molecule level, parameters like polymer backbone planarity, side chain length, conjugation length, and reorganization energies [32] may influence the conductivity. The interactions between analytes and polymers most likely modulate one or more of these parameters, thus modulating the current density through the thin film polymers. This implies the possibility of multiple sensing mechanisms acting at the same time. Upon exposure of a specific polymer to a particular analyte, one mechanism possibly dominates the others, resulting in either a conductivity increase or decrease. As the microstructure is changed, by choice of polymer chemical construction or even by film processing conditions, the potential dominant sensing mechanism may change. In the following we propose some specific sensing mechanisms for the rr-PT polymers resulting from their different molecular structures.
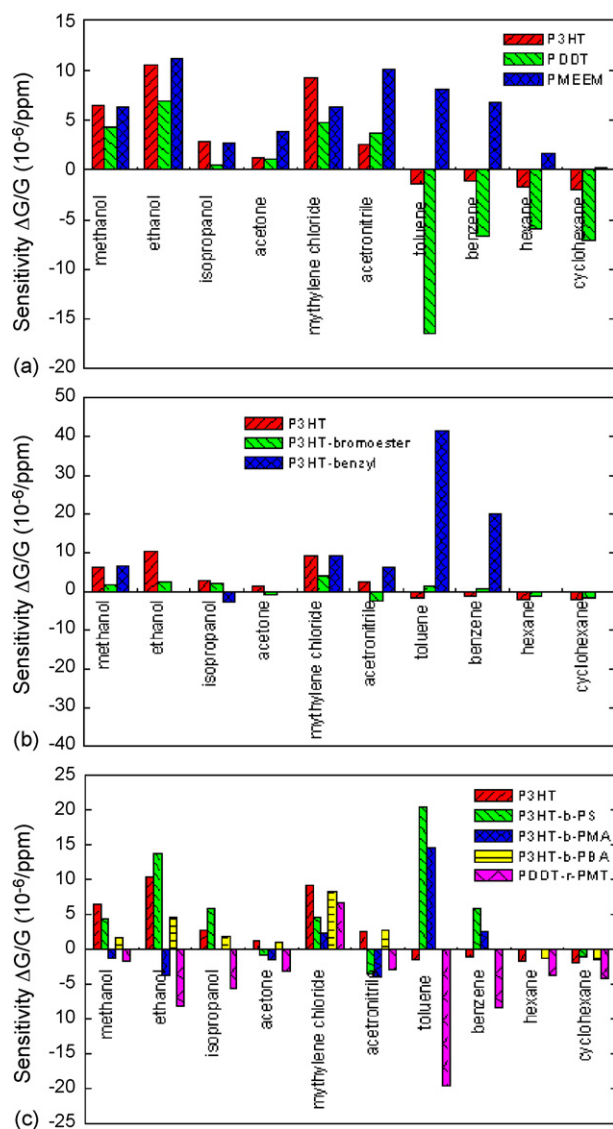
Fig. 7. Molecular structure effects on response pattern: (a) side chain effects, (b) end group effects and (c) copolymer effects.

4.1. Side chain effects

The response patterns of P3HT, PDDT and PMEEM polymers, which have different side chains, are shown in Fig. 7(a). P3HT and PDDT both have an alkyl side chain, and correspondingly they show similar response patterns. Both polymers produce a positive response to polar analytes and a negative response to non-polar analytes. One possible explanation is that the dipole–dipole electrostatic force between polar analytes with certain dipole moments and polymer dipolar alkyl side chains can push the polymer molecules closer together, thus reducing the hopping distances and energy. This would result in a conductance increase. In contrast, non-polar analytes such as toluene and benzene, which are actually solvents for these polymers, dissolve into the polymer and separate the polymer molecules and film microstructures. Hence, the carrier hopping distance and barrier energy increase and conductivity decreases. This 'swelling' effect is also observed in other types

of polymer sensors such as carbon black composites [11]. Also, PDDT showed a much stronger response to non-polar analytes than did P3HT. This is probably because a longer side chain could result in a more open structure, and hence, more room for analyte absorption.

PMEEM, which has a side chain containing oxygen atoms, showed a positive response to all VOCs. Due to the oxygen atoms in PMEEM, the side chain of PMEEM has a much higher dipole moment than the alkyl side chains in P3HT and PDDT. Therefore, stronger electrostatic interactions occurred when PMEEM polymer was exposed to all tested analytes. It is plausible this is why PMEEM generally shows a positive response to the VOCs.

4.2. End group effects

The response patterns of P3HT, P3HT-benzyl, and P3HT-bromoester polymers, which have different end groups, are shown in Fig. 7(b). While the P3HT-bromoester and P3HT showed a small response to toluene and benzene, P3HT-benzyl showed a large positive response. Toluene and benzene are non-polar molecules with a very small or zero dipole moment. This means the previously described dipole interaction does not apply. Since the benzyl end group has a benzene ring, it is plausible that the induced van der Waals force is the main interaction between analytes and end groups with a similar structure to the analytes. This interaction is attractive; thus, it brings the polymer molecules closer together and reduces the charge hopping distance. Therefore, the conductivity in P3HT-benzyl increases upon exposure to toluene and benzene. For the other two non-polar analytes, hexane and cyclohexane, the polymer showed no response.

4.3. Copolymers

The sensing properties of copolymers depend on the structure of the secondary polymer chain as well as the primary chain. For example, PHT-b-PS shows a strong positive response to toluene and benzene, which are solvents for polystyrene and also have a similar chemical structure to the side chain of polystyrene. Again, it is likely that the induced van der Waals force tends to bring the similar chemical structures closer together, which reduces the charge carrier hopping distance and energy, causing an increase in conductivity.

The PDDT-r-PMT polymer, in which the secondary chain was inserted inside the primary polymer in random segment lengths, showed a negative response for most VOCs. This suggests that the interaction of the analyte molecules and alternating side groups might twist the copolymer molecules and reduce the polymer chain conjugation length. Thus, the electronic coupling between adjacent monomer units is interfered with and the current density along the molecule chain decreases [33].

5. Conclusion

Sensors based on arrays of rr-PT chemresistors were demonstrated to be viable options for detection and discrimination of VOCs. The family of rr-PT-based conductive polymers and

copolymers with various side chains and end groups were synthesized and tested. Their responses showed a variety of distinct new patterns that might significantly enhance sensor discrimination capability between VOCs. Possible sensing mechanisms and interactions between the VOC vapors and the variety of rr-PT chemistries that might account for the observed electrical property changes were described. This work provides the foundation for further research and development to design chemical structures to optimally respond to a given analyte. Also, while we anticipate the sensor response to be both humidity and temperature dependent this analysis represents a significant effort. We have just begun this and hope to present these results in a later publication.

Acknowledgements

References

[1] A.K. Srivastava, Detection of volatile organic compounds (VOCs) using SnO_2 gas-sensor array and artificial neural network, Sens. Actuators B 96 (2003) 24–37.

[2] B. Li, S. Santhanam, L. Schultz, M. Jeffries-EL, M.C. Iovu, G. Sauvé, J. Cooper, R. Zhang, J.C. Revelli, A.G. Kusne, J.L. Snyder, T. Kowalewski, L.E. Weiss, R.D. McCullough, G.K. Fedder, D.N. Lambeth, Volatile organic compound discrimination using nanostructured polythiophene sensors, Proc. IEEE Sens. 2005 (2005) 191–194.

[3] S. Hamilton, M.J. Hepher, J. Sommerville, Polypyrrole materials for detection and discrimination of volatile organic compounds, Sens. Actuators B 107 (2005) 424–432.

[4] L. Han, X. Shi, W. Wu, F.L. Kirk, J. Luo, L. Wang, D. Mott, L. Cousineau, S.I.-I. Lim, S. Lu, ZhongF C.-J., Nanoparticle-structured sensing array materials and pattern recognition for VOC detection, Sens. Actuators B 106 (2005) 431–441.

[5] E.S. Snow, F.K. Perkins, E.J. Houser, S.C. Badescu, T.L. Reineche, Chemical detection with a single-walled carbon nanotube capacitor, Science 307 (2005) 1942–1945.

[6] K.S. Suslick, N.A. Rakow, A. Sen, Colorimetric sensor arrays for molecular recognition, Tetrahedron 60 (2004) 11133–11138.

[7] Y.S. Kim, S.-C. Ha, Y. Yang, Y.J. Kim, S.M. Cho, H. Yang, Y.T. Kim, Portable electronic nose system based on the carbon black-polymer composite sensor array, Sens. Actuators B 108 (2005) 285–291.

[8] H. Liu, J. Kameoka, D.A. Czaplewshi, H.G. Craighead, Polymeric nanowire chemical sensor, Nanoletter 4 (2004) 671–675.

[9] D.M. Wilson, S. Hoyt, J. Janata, K. Booksh, L. Obando, Chemical sensors for portable, handheld field instruments, IEEE Sens. J. 1 (2001) 256–274.

[10] N. Bârsan, U. Weimar, Understanding the fundamental principles of metal oxide based gas sensors; the example of CO sensing with SnO_2 sensors in the presence of humidity, J. Phys.: Condens. Matter 15 (2003) 813–839.

[11] M.C. Lonergan, E.J. Severin, B.J. Doleman, S.A. Beaber, R.H. Grubbs, N.S. Lewis, Array-based vapor sensing using chemically sensitive, carbon black-polymer resistors, Chem. Mater. 8 (1996) 2298–2312.

[12] Z. Bao, A. Dodabalapur, A.J. Lovinger, Soluble and processable regioregular poly(3-hexylthiophene) for thin film field-effect transistor applications with high mobility, Appl. Phys. Lett. 69 (1996) 4108–4110.

[13] H. Sirringhaus, N. Tessler, R.H. Friend, Integrated optoelectronic devices based on conjugated polymers, Science 280 (1998) 1741–1744.

[14] R.S. Loewe, S.M. Khersonsky, R.D. McCullough, A simple method to prepare head-to-tail coupled, regioregular poly(3-alkylthiophenes) using grignard metathesis, Adv. Mater. 11 (1999) 250–253.

[15] R.D. McCullough, M. Jayaraman, The tuning of conjugation by recipe: the synthesis and properties of random head-to-tail poly(3-alkylthiophene) copolymers, J. Chem. Soc. Chem. Commun. 2 (1995) 135–136.

[16] M.C. Iovu, M. Jeffries-EL, E.E. Sheina, J.R. Cooper, R.D. McCullough, Regioregular poly(3-alkylthiophene) conducting block copolymers, Polymer 46 (2005) 8582–8586.

[17] M. Jeffries-EL, G. Sauvé, R.D. McCullough, In-situ end-group functionalization of regioregular poly(3-alkylthiophene) using the Grignard metathesis polymerization method, Adv. Mater. 16 (2004) 1017–1019.

[18] L. Zhai, R.L. Pilston, K.L. Zaiger, K.K. Stokes, R.D. McCullough, A simple method to generate side-chain derivatives of regioregular polythiophene via the GRIM metathesis and post-polymerization functionalization, Macromolecules 36 (2003) 61–64.

[19] B. Crone, A. Dodabalapur, A. Gelperin, L. Torsi, H.E. Katz, A.J. Lovinger, Electronic sensing of vapors with organic transistors, Appl. Phys. Lett. 78 (2001) 2229–2231.

[20] L. Torsi, A. Tafuri, N. Cioffi, M.C. Gallazzi, A. Sassella, L. Sabbatini, P.G. Zambonin, Regioregular polythiophene field-effect transistor employed as chemical sensors, Sens. Actuators B 93 (2003) 257–262.

[21] R.D. McCullough, G. Sauvé, B. Li, M. Jeffries-EL, S. Santhanam, L. Schultz, R. Zhang, M.C. Iovu, J. Cooper, P. Sreedharan, J.C. Revelli, A.G. Kusner, T. Kowalewski, J.L. Snyder, L.E. Weiss, D.N. Lambeth, G.K. Fedder, Regioregular polythiophene nanowires and sensors, Proc. SPIE 5940 (2005) 28–34.

[22] L. Burgi, T.J. Richards, R.H. Friend, H. Sirringhaus, Close look at charge carrier injection in polymer field-effect transistors, J. Appl. Phys. 94 (2003) 6129–6137.

[23] A. Bietsch, J. Zhang, M. Hegner, H.P. Lang, C. Gerber, Rapid functionalization of cantilever array sensors by inkjet printing, Nanotechnology 15 (2004) 873–880.

[24] H. Sirringhaus, T. Kawase, R.H. Friend, W. Wu, E.P. Woo, High-resolution inkjet printing of all-polymer transistor circuits, Science 290 (2000) 2123–2126.

[25] L.E. Weiss, L. Schultz, E. Miller, Inkjet deposition system with computer vision-based calibration for targeting accuracy, Carnegie Mellon University Technical Report CMU-RI-TR-06-15, 2006.

[26] L. Torsi, A.J. Lovinger, B. Crone, T. Someya, A. Dobabalapur, H.E. Katz, A. Gelperin, Correlation between oligothiophene thin film transistor morphology and vapor responses, J. Phys. Chem. B 106 (2002) 12563–12568.

[27] R. Zhang, B. Li, M.C. Iovu, M. Jeffries-EL, G. Sauvé, J. Cooper, S. Jia, S. Tristram-Nagle, D.M. Smilgies, D.N. Lambeth, R.D. McCullough, T. Kowalewski, Nanostructure dependence of field-effect mobility in regioregular poly(3-hexylthiophene) thin film field effect transistors, J. Am. Chem. Soc. 128 (2006) 3480–3481.

[28] R.D. Deegan, O. Bakajin, T.F. Dupont, G. Huber, S.R. Nagel, T.A. Witten, Capillary flow as the cause of ring stains from dried liquid drops, Nature 389 (1997) 827–829.

[29] B.-J.d. Gans, U.S. Schubert, Inkjet printing of well-defined polymer dots and arrays, Langmuir 20 (2004) 7789–7793.

[30] E. Johansson, S. Larsson, Electronic structure and mechanism for conductivity in thiophene oligomers and regioregular polymer, Synth. Met. 144 (2004) 183–191.

[31] T. Someya, H.E. Katz, A. Gelperin, A.J. Lovinger, Vapor sensing with α,ω-dihexylquarterthiophene field-effect transistors: the role of grain boundaries, Appl. Phys. Lett. 81 (2002) 3079–3081.

[32] G.R. Hutchison, M.A. Ratner, T.J. Marks, Hopping transport in conductive heterocyclic oligomers: reorganization energies and substituent effects, J. Am. Chem. Soc. 127 (2005) 2339–2350.

[33] F.C. Grozema, V.D. Piet Th, Y.A. Berlin, M.A. Ratner, L.D.A. Siebbeles, Intramolecular charge transport along isolated chains of conjugated polymers: effect of torsional disorder and polymerization defects, J. Phys. Chem. B 106 (2002) 7791–7795.

Biographies

Bo Li received his B.S. and M.S. in electrical engineering from Xi'an Jiaotong University in 1999 and 2002. He is currently pursuing a Ph.D. degree in electrical and computer engineering at Carnegie Mellon University. His research interests include chemical sensors, molecular electronics, analog IC and MEMS.

Suresh Santhanam is a process engineer in the department of electrical and computer engineering at Carnegie Mellon University. He has been with the university for over 20 years after receiving his M.Sc. degree. He is the author of over 18 papers in technical journals and also has two patents to his name.

Lawrence Schultz is a senior research engineer at the Robotics Institute, Carnegie Mellon University.

Malika Jeffries-EL received her BA from Wellesley College and her masters and doctoral degrees from The George Washington University. She then worked at Carnegie Mellon University as a post-doctoral research fellow under the direction of Prof. Richard D. McCullough. In the fall of 2005 she took her current position as an assistant professor in the department of chemistry at Iowa State University.

Mihaela C. Iovu holds a Ph.D. degree in polymer chemistry from Politechnica University of Bucharest (Romania). Her research interests include the design and synthesis of novel semiconducting polymers with tunable optical and electrical properties.

Genevieve Sauvé obtained her Ph.D. at the California Institute of Technology in 1999, working with Prof. Nathan S. Lewis on dye-sensitized solar cells. She then took a position as senior development chemist at PPG Industries. In 2002, she joined Prof. Richard D. McCullough's group at Carnegie Mellon University, where she is now a research associate. Her interests include conductive polymers, organic field effect transistors and organic photovoltaics.

Jessica Cooper received her B.S. degree in chemistry (2002) from the University of Pittsburgh at Johnstown and a M.S. degree in chemistry (2004) from Carnegie Mellon University. Currently she is a chemistry Ph.D. candidate at Carnegie Mellon University where her research focuses on the synthesis and characterization of polythiophene and its derivatives.

Rui Zhang holds a B.E. degree in polymer science and engineering and M.S. degree in chemistry from Jilin University (PR China). He is a Ph.D. student in chemistry program at Carnegie Mellon University where his interests include proximal probe technique, organic thin film device design and analysis, and X-ray scattering of organic thin film with well-defined nanostructures.

Joseph C. Revelli holds a degree in chemical engineering from Carnegie Mellon University (2006) and is a Ph.D. student in Biochemistry at Emory University.

Aaron G. Kusne is a Ph.D. candidate in electrical and computer engineering at Carnegie Mellon University, where he received his M.S. degree. He is currently working on nanostructured carbon for electrical devices with a focus on field emission. His research interests include understanding conduction and field emission mechanics for nanostructured carbon.

Jay L. Snyder received his B.S. in chemical engineering from West Virginia University and a M.S. in Occupational Health from the University of Pittsburgh's Graduate School of Public Health. Presently, he is developing a program for end-of-service life detection for personal protective equipment. This program is a part of the U.S. Center for Disease Control/National Institute for Occupational Safety and Health's mission to improve worker's safety and health.

Tomasz Kowalewski received his Ph.D. from Polish Academy of Sciences in 1988 and is presently an associate professor of Chemistry at Carnegie Mellon University. His current research interests include physical chemistry of macromolecules with the emphasis on macromolecular self-assembly, soft condensed matter, organic conductors and semiconductors, nanostructured carbons and proximal probe techniques.

Lee E. Weiss is a research professor in the Robotics Institute of Carnegie Mellon University. He obtained his M.Sc. in bioengineering and Ph.D. in electrical and computer engineering from Carnegie Mellon. His current research interests include biological and chemical sensors and tissue engineering.

Richard D. McCullough is the Dean of the Mellon College of Science, Carnegie Mellon University, Pittsburgh, PA. Dr. McCullough is also a professor with the Department of Chemistry. He received his B.S. in chemistry in 1982 from the University of Texas at Dallas and his Ph.D. in Organic Chemistry in 1988 from The Johns Hopkins University, Baltimore, MD. Dr. McCullough began his career at Carnegie Mellon University as a assistant professor in 1990, became an associate professor in 1995, Associate Department Head 1996, professor in 1998, Department Head of Chemistry 1998 and Dean of the Mellon College of Science, 2001. His current research interests range over organic, polymer, and inorganic materials chemistry, including the self assembly and synthesis of highly conductive organic polymers and oligimers, conjugated polymer sensors, nanoelectronic assembly and fabrication of molecular circuits and transistors, new designs methods and the synthesis of organic–inorganic hybrid nanomagnets and high-spin materials, crystal engineering and novel nanocrystalline semiconductor materials.

Gary K. Fedder is the Howard M. Wilkoff professor of electrical and computer engineering at Carnegie Mellon University and holds a joint appointment with the Department of Electrical and Computer Engineering and The Robotics Institute. He is also the Director of the Institute for Complex Engineered Systems. He received B.S. and M.S. degrees in electrical engineering from MIT in 1982 and 1984, respectively. From 1984 to 1989, he worked at the Hewlett-Packard Company on circuit design and printed-circuit modeling. In 1994, he obtained a Ph.D. degree from U.C. Berkeley. His research interests include microsensor and microactuator design and modeling, integrated MEMS manufactured in CMOS processes and structured design methodologies for MEMS.

David N. Lambeth received his B.S. in Electrical Engineering from the University of Missouri in 1969 and his Ph.D. from the Massachusetts Institute of Technology in 1973. Before becoming a professor of electrical and computer engineering and material science and engineering at Carnegie Mellon University in 1989 he worked at the Eastman Kodak Company Research Laboratories for 15 years and, for a short while, at the Control Data Corporation. He has been involved in sensor research for over 25 years. His research interests include physical and chemical sensors, transducers, MEMS, RF devices, thin film materials, magnetism, and data storage systems.